Overview: Electron Cloud Trapping in High Energy Accelerators

1.1 Objective and Significance

The electron cloud (EC) effect is a well-known phenomenon in particle accelerators (see, for example,[1]), in which a high density of low energy electrons builds up inside the vacuum chamber. These electrons can cause a wide variety of undesirable effects, including emittance growth and beam instabilities[2]. Electron cloud has been observed in many facilities[3], and is expected to be a major limiting factor in next generation positron and proton storage rings.

Performance of the B-Factory storage rings KEK-B in Japan [4] and PEP-II in the U.S. [5] was limited at least in part by electron cloud effects. Electron cloud induced pressure rise and beam instabilities were observed in the CERN Proton Synchrotron, part of the injection chain for the Large Hadron Collider (LHC). Electron cloud phenomena limit bunch spacing in the LHC, increase heat load on cold dipoles, and lead to bunch dependent emittance growth and poor lifetime[3]. An understanding of these effects is essential for the LHC luminosity upgrade, as well as future electron positron colliders.

The decay time of the electron cloud dictates the length of the gap that separates bunch trains. Longer decay times imply a longer gap, with the length of the gap ultimately limiting the beam current. Typical decay times for electron clouds in drifts and dipole fields are about 100 ns. However electrons can be trapped in quadrupole and sextupole fields for times long compared to the revolution period of the ring, essentially indefinitely. Electron trapping was observed in the CESR dipole magnets that are equipped with distributed ion pumps, where the electric fields from the pumps combine with the dipole magnetic field to trap electrons [7]. Trapping of electrons in a proton storage ring was reported in Ref. [6].

The first evidence of electron trapping in the field of a quadrupole of a positron storage ring appeared at the Cornell Electron Storage Ring (CESRTA) in 2013 [13]. Cloud with lifetime well in excess of the order 2 micro-second revolution period of the storage ring was measured in the quadrupole chamber. Simulations indicated that electrons in the chamber would be trapped indefinitely. The trapping phenomenon has important implications for high intensity rings. Trapping of photoelectrons in the quadrupole and sextupole magnets of the Super KEK-B positron ring has been modeled [8] in some detail and has motivated vacuum chamber redesign. Estimates of long-lived electron cloud buildup in quadrupoles at the LHC indicate significant consequences for cryogenic heat load [9]. Simulations suggest that trapping occurs with electron beams as well as for positron and proton beams, and might impact performance of very low emittance and high brightness electron storage rings for X-ray science.

Our measurements with a time-resolving electron detector located in a quadrupole magnetic field have provided comparisons of signals from 10- and 20-bunch trains of positrons which show clear evidence for electron trapping during the entire 2.3 μs time interval prior to the return of the bunch train. Modeling indicates that approximately 7% of the cloud generated by a 5.3 GeV train of 20 bunches, each carrying 1.3×10^{11} positrons, remains trapped. The measurements show a non-monotonic dependence on bunch spacing indicative of beam-induced multipacting effects. The clearing effect of an intermediate bunch has been measured and successfully modeled, showing the trapped cloud can be reduced by a factor of four by such a clearing bunch. The characteristic of a quadrupole magnetic field to concentrate electrons near the beam raises concerns for storage rings with positively charge beams, since those electrons can be attracted into the beam.

The goal of this proposal is to further our understanding of the growth and decay of the electron cloud in quadrupole fields with better measurements. Specifically we propose to determine:

- Dependence of cloud properties on quadrupole field strength for gradients from 0 through

3.5 T/m with positron beams.

- Dependence of cloud properties on quadrupole field strength for gradients from 0 through 3.5 T/m with electron beams (A first time measurement).
- Dependence of cloud density on bunch charge to test the specific prediction that at large bunch charge there is a disproportionate increase in the EC density and in the azimuthal distribution of the electron flux onto the beam-pipe wall.
- Measurements of time-resolved electron cloud growth and decay using two independents detection techniques. Resonant microwave measurements will provide information about the density of the cloud within the volume of the chamber. A time resolving shielded electrode will measure the flux of electrons into the wall of the chamber.
- The dependence of the effectiveness of a clearing bunch, on quadrupole gradient and beam species.

In lepton machines and high energy proton accelerators, the cloud is seeded by photoelectrons generated by synchrotron radiation. The collision of these electrons with the beam pipe can then produce one or more secondary electrons, depending on the secondary electron yield (SEY) of the material. If the average SEY is greater than unity, the cloud density will grow exponentially, until a saturation is reached.

The study of EC growth, decay and mitigation has been carried out as part of the CESR storage ring test accelerator (CESRTA) program [10]. Specialized instrumentation includes a variety of detectors that sample the flux of electrons onto the beam-pipe wall. Some measure a DC current, while others give the time-resolved flux of electrons onto the wall. Data from these instruments have been compared with codes that simulate electron cloud growth such as ECLOUD [11] and POSINST [12]. The codes have been extended to incorporate response of the electron detectors. These comparisons have led to refinement of the codes, so that they better predict behavior of the next generation high intensity accelerators.

The trapping phenomenon was observed by accelerator scientists Crittenden and Sikora with students, using a shielded electrode detector in a quadrupole at the CESR storage ring that samples the time-resolved flux of cloud electrons onto the beam-pipe surface. Data from this detector have demonstrated for the first time that a fraction of the electron cloud is trapped in the quadrupole [13]. Simulations of the cloud using the ECLOUD code are in rough agreement with the measured signals generated by a positron beams.

However the quality of our measurements of the behavior of the electron cloud in a quadrupole was limited by the low signal levels and our inability to vary the quadrupole gradient. Indeed with an electron beam, the intensity of the synchrotron radiation is insufficient to produce a signal in this location. The proposed new instrumentation will overcome the limitations of the existing hardware, allowing a more complete characterization of electron cloud trapping in quadrupoles, as enumerated in the above list of goals.

The research will be carried out within the framework of the CESRTA program, which is funded by NSF 1416318 Cornell Program for Student-Centered Accelerator Science (9/1/2014-8/31/2017). Students (graduate and undergraduate) and post docs participating in the proposed study of trapped cloud will be supported by the existing grant and the REU program. The CESRTA organization will provide overall coordination of the design, fabrication and installation of the equipment. The concept for the electron cloud detection, detailed design of the detectors, and electron cloud and RF microwave analysis all borrow heavily from the CESRTA program experience and expertise.

2 Proposed Instrumentation

We propose that a new quadrupole with a shielded electrode detector be installed in a section of the storage ring that has higher synchrotron radiation flux, especially with electron beams. Improvements will be made in the design of the detector, including an azimuthally wider collector that simulations predict will give a significantly higher sensitivity at high bunch currents. By adding a new quadrupole and detector near an existing quadrupole it will be possible to vary the quadrupole field strength with a stored beam, compensating for this field change primarily with the adjacent quadrupole. The power supplies for the quadrupoles are independent, allowing the possibility of measuring the dependence of the trapped cloud density on the quadrupole gradient from zero up to at least 3.5 T/m. In addition, the new quadrupole chamber will be designed with electrodes to enable resonant microwave measurements of cloud density. The technique of using resonant microwaves to measure the EC density within the beam-pipe volume has been developed at CESR by Sikora (see for example [19]) and demonstrated at various locations around the storage ring. The EC densities obtained with this method have been compared with those obtained using both DC current and time-resolving wall flux detectors [15], mostly in sections without external magnetic fields. Analysis and cross-calibration of the data from the time resolving detector with the microwave measurements will provide a better understanding of the instruments as well as the temporal nature of the cloud. Measurements in the presently instrumented quadrupole chamber using this technique are not possible, primarily because there are no electrodes that might be used to couple microwaves into the chamber. Sikora and Crittenden will lead the effort to design the new instrumentation and carry out the experimental program.

2.1 New Quadrupole Magnet and Detectors

The existing quadrupole with EC detector (Q48W) is located in a straight section approximately four meters from the nearest upstream dipole for the positron beam and 14 m from the nearest upstream dipole for the electron beam. Both dipoles are so-called 'soft bends' with a relatively low field of about 1.4 kG for a 5.3 GeV beam. We propose to install a new quadrupole with detector in a region of the storage ring where the synchrotron radiation flux on the vacuum chamber will be significantly higher. The 3.7 m (Q15W) straight is between dipole magnets with 2.24 kG(electrons) and 3.36 kG(positrons) fields respectively. The instrumented quadrupole will be located in this straight adjacent to a standard lattice quadrupole. Figs. 1 and 2 compare the initial estimates of the flux of synchrotron radiation for electron and positron beams at the old (existing) and new (proposed) detector locations.

The direct synchrotron light flux from a positron and electron beam at Q15W is significantly higher than at the present location of Q48W. This increase in flux will give better signal to noise for measurements with positrons and allow the possibility of measurements with electron beams. Simulations with the ECLOUD code of the expected signal from the detector at the new location show similar signals for 5.3 GeV beams and quadrupole gradients of 7.5 T/m and 3.5 T/m as well as for 2 GeV beams with gradients of 2 T/m.

The new quadrupole will be assembled from existing CESR MK1 style laminations. In order that the aperture be large enough to house the flux detector, the laminations will be machined and spacers added to give a 15 cm clearance for the beam-pipe/detector assembly. This modification is identical to that made to a quadrupole that has been in service for the past 10 years in the context of a luminosity monitor[16].

A new shielded electrode detector will be based on the existing design described in Ref. [13]. Simulations show that the azimuthal distribution of the peak electron flux increases with bunch

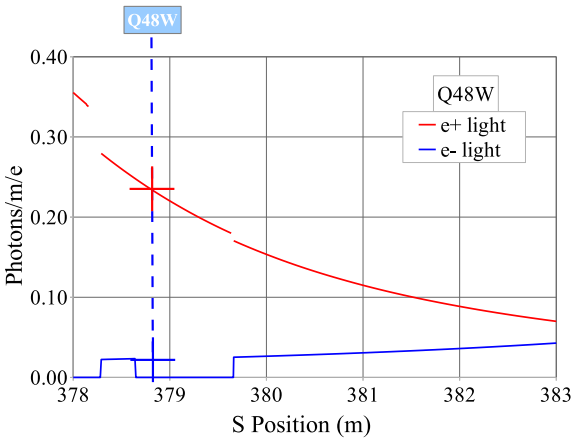

Figure 1: At the present location (Q48W) of the quadrupole equipped with an EC detector, the synchrotron light flux at 5.3 GeV is about 0.23 photons/m/electron for a positron beam and nearly zero for an electron beam.

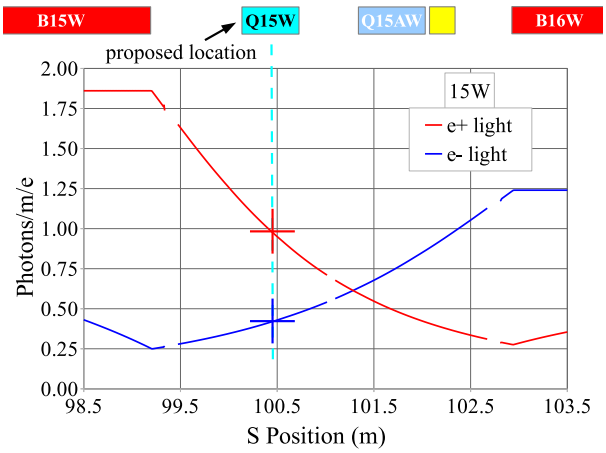

Figure 2: At the proposed location of a new quadrupole with EC detector (Q15W), there is higher synchrotron light flux than at the present Q48W location for both positron and electron beams at 5.3 GeV.

charge and with the highest anticipated charge, it will extend beyond the 6 mm width of the existing detector. A wider azimuthal acceptance will be part of the new detector design. The new detector and quad will replace an existing 120 cm test section of beam-pipe instrumented with flux detectors in a drift [14]. As shown in Fig. 2 the new quadrupole will be adjacent to a standard lattice quadrupole. Variations in the field in the instrumented quad can be compensated with its neighbor allowing first measurements of the dependence on magnet gradient. The readout electronics and cabling for the existing electron flux detector will be reused.

The microwave properties of the new quadrupole chamber, including identificaton of resonant modes, will be modeled with Inventor^{TM} and CST Microwave Studio^{TM}. Button electrodes to couple microwaves in and out of the chamber will be included in the design. The simulation will be benchmarked with bead-pull measurements on approximate physical models and on the final assembly before installation in the storage ring. For data taking, two runs of Heliax will be needed for the drive and pickup signals and an existing signal generator and spectrum analyzer will be used.

2.2 Description of Electron Cloud Detectors

The proposed EC density detectors are extensions of devices already in use at CESRTA. The following sections give a brief description of these detectors.

2.2.1 Shielded Electrode in a Quadrupole Magnet

A sketch of the existing shielded electrode detector is shown in Fig. 3. An array of parallel holes allows cloud electrons to enter the detector that is centered on a pole face near the longitudinal center of the quadrupole. The holes have a depth to diameter ratio of 3:1, which attenuates the electromagnetic pulse from the passing bunch, while providing adequate transparency for electrons. The collector is about 6 mm wide by 100 mm long and is AC coupled to 40 dB of amplification before the signal is recorded with a digital oscilloscope.

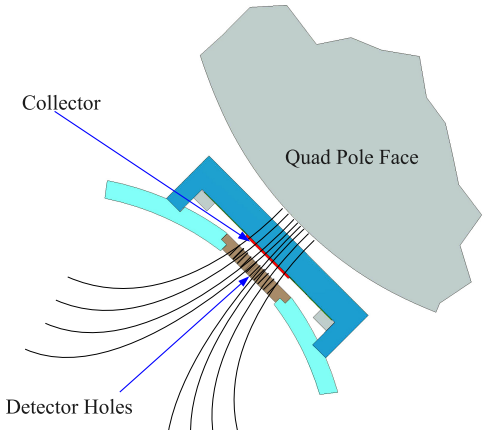

Figure 3: A sketch of the quadrupole shielded electrode, where holes in the beam-pipe wall allow cloud electrons to enter the detector, while attenuating the direct beam signal.

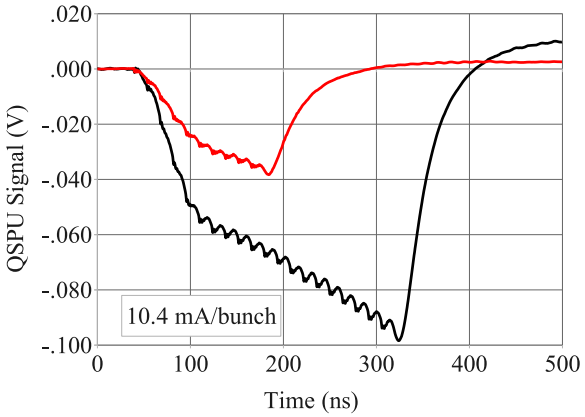

Figure 4: Quadrupole shielded electrode data from a 10-bunch train and a 20-bunch train of positrons at 10 mA/bunch (1.6×10^{11} positrons/bunch).

Figure 4 shows the data obtained with this detector that was the first indication of trapped charge. Data from two bunch configurations are shown, a 10-bunch and a 20-bunch train with the same charge per bunch, plotted on the same scale. The signal from the first ten bunches of the 20-bunch train is larger than the signal from the 10-bunch train alone. This suggests that the 20-bunch train leaves some amount of charge behind that is available to seed the buildup of the cloud on the next turn. Additional information on this and similar measurements is given in Ref. [13].

According to simulations with the ECLOUD code, roughly 7% of the EC density remains trapped in the quadrupole field for times longer than the 2562 ns revolution period of the stored beam in CESR [17]. Figure 5 shows the simulated density in a cross-section of the beam-pipe at a time just before the return of a stored 20-bunch train of positrons with bunch populations of 1.16×10^{11} and 1.32×10^{11}. Simulations also suggest that at the highest bunch charge, the peak current of electrons onto the beam-pipe wall is split about the line centered on the pole face. Figure 6 shows the simulated distribution of electrons just after the passage of a 20-bunch train of positrons. At the highest bunch charge, the split distribution is wider than the acceptance of the 6 mm width of the present detector, reducing its sensitivity to the increased flux of electrons at these currents. The original 6 mm width design, was based on the assumption of a narrow distribution of low energy cloud electrons that would spiral along the field lines toward the pole face. The 3:1 depth to diameter ratio of the holes limited the acceptance of the detector for electrons incident at larger angles. Our redesign will include a wider collector and an array of holes oriented to more nearly follow the diverging field lines of the quadrupole.

2.2.2 Microwave Measurements

The use of resonant microwaves to measure electron cloud (EC) density has been developed by Sikora and students at Cornell over the past several years [19]. In this technique, the accelerator beam-pipe is excited with microwaves near the cutoff frequency of the pipe, typically with some resonant response as shown in the example of Fig. 7. The presence of the electron cloud will shift the resonant frequencies by an amount $\Delta\omega$ given by Eq. 1 in the limit of EC densities with low

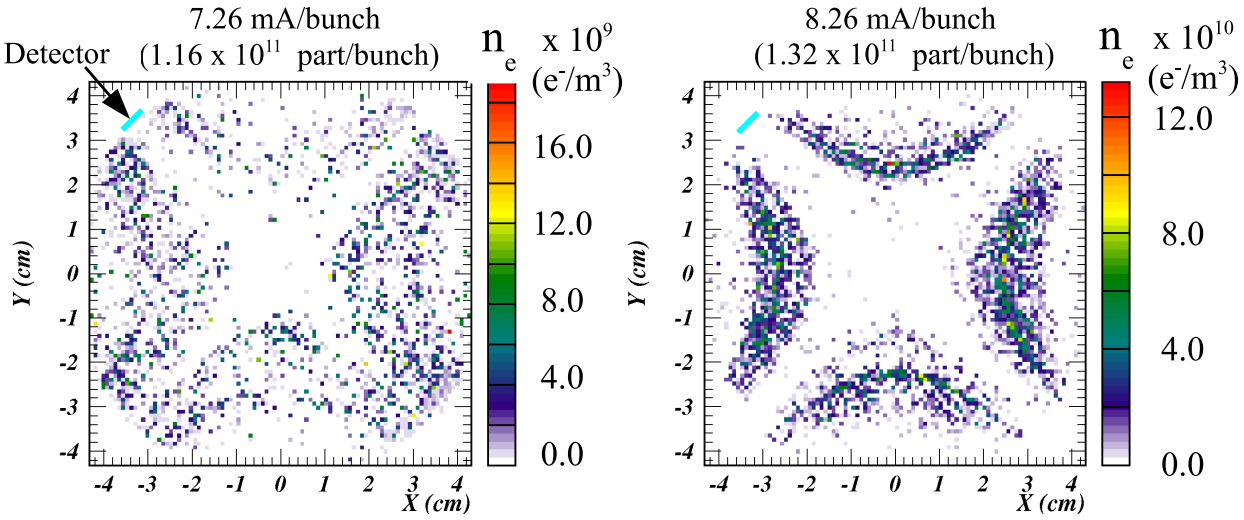

Figure 5: ECLOUD simulations show cloud electrons that are trapped in the quadrupole field at a time just before the return of a stored 20-bunch train of positrons. The revolution period is 2562 ns.

collision frequency. In this equation, n_e is the local EC density, E_0^2 the local electric field of the resonant microwaves, ε_0 the vacuum permittivity, and with e and m_e the charge and mass of an electron. The integrals are taken over the resonant volume.

$$\frac{\Delta\omega}{\omega_0} \approx \frac{e^2}{2\varepsilon_0 m_e \omega_0^2} \frac{\int_V n_e E_0^2 dV}{\int_V E_0^2 dV} \tag{1}$$

In principle, a time-averaged EC density can be obtained by measuring shifts in the resonant peak frequencies, but at densities of 10^{12} e^-/m^3, $\Delta\omega/\omega$ is only about 10^{-4} and is not easily measured given the typically low Q values. In addition, changes in beam-pipe temperature will effect the resonant frequency. Instead, we use a short train of bunches in the storage ring to generate a periodic EC density. Figure 8 shows that when the beam-pipe is excited at or near a resonant frequency, the periodic EC density will generate phase modulation in the response. The phase modulation sidebands are then observed with a spectrum analyzer [19].

An alternate technique is to detect the change in phase directly and record it with an oscilloscope [20]. The development of this phase detection technique will be important for the study of electron cloud that is trapped on a timescale that is long compared to the revolution period of the storage ring. The trapped cloud does not generate a modulation signal, but does produce a phase offset. With careful analysis, the phase signal will provide a more direct measure of the time evolution of the cloud.

3 Activities

3.1 Design

- Design new shielded electrode flux detector with larger azimuthal acceptance.
- Design the chamber geometry to support microwave measurements.

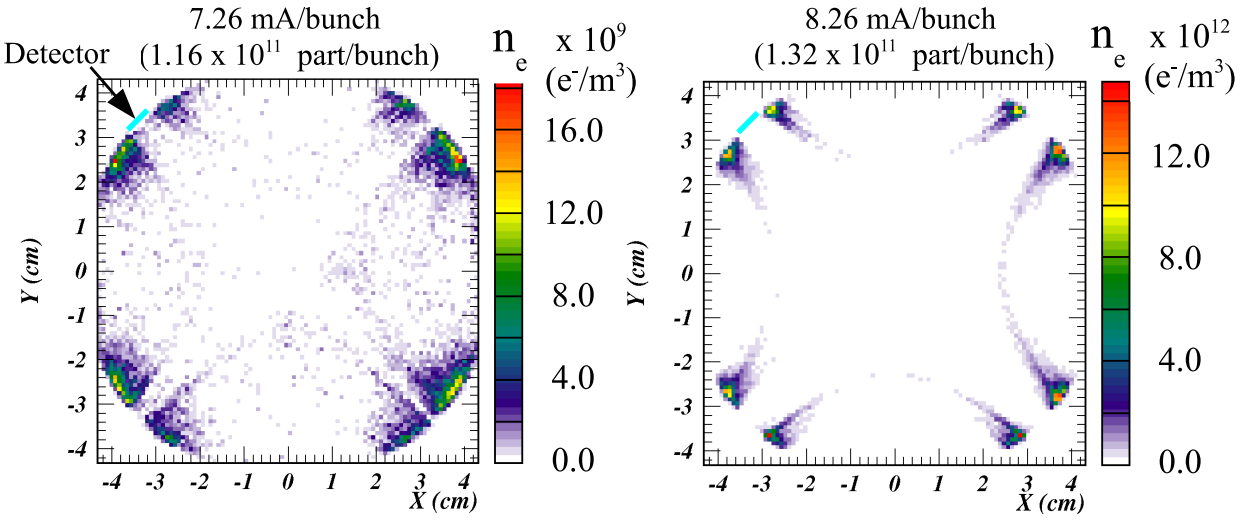

Figure 6: ECLOUD simulations at a time just after the passage of a 20-bunch train of positrons show that the electrons hitting the beam-pipe wall (and detector) are split about the center of the quadrupole pole face. This is especially true at the highest bunch population of 8.26 mA/bunch. The existing detector is 6 mm wide at the approximate scale and location shown. The new detector will cover a wider azimuth to improve signal electron acceptance at the higher bunch populations.

- Design the mechanical support structures that will be needed for the installation of the quadrupole magnet and beam-pipe.
- Plan the location and routing of magnet power, signal cables and instruments for data collection.

3.2 Fabrication

- Large aperture quadrupole
  - Machine the pole tips of the assembled laminations and the iron spacers.
  - Wind coils, install them on the poles and make electrical, magnetic field quality and water flow tests.
  - Machine and assemble the mechanical support for the quadrupole
- Shielded electrode flux detector
  - Fabricate the shielded electrode detector, the hole array plates and machine slots in the beam-pipe.
  - Assemble these onto the beam-pipe; perform vacuum and electrical tests.
- Resonant microwave detector
  - Machine and assemble button electrodes for coupling microwaves in and out of the chamber
  - Perform bead pull measurements of quadrupole chamber to characterize resonant modes.

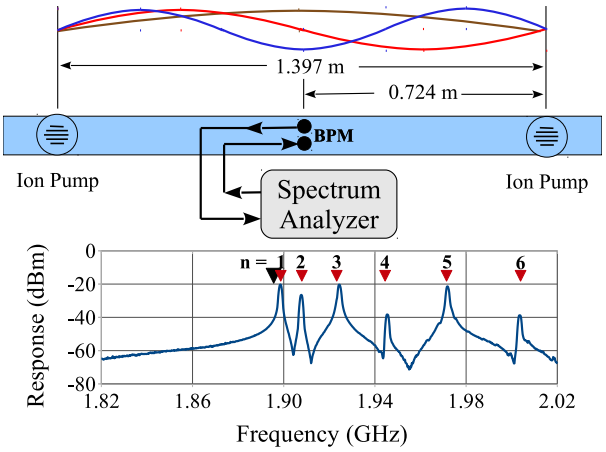

Figure 7: An example of resonant response of CESR beam-pipe. The triangles mark the resonant frequencies calculated for a shorted section of waveguide of length 1.385 m with a cutoff frequency of 1.8956 GHz.

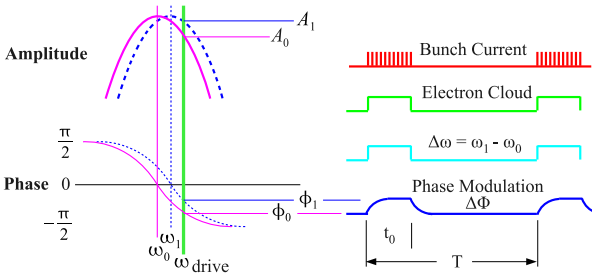

Figure 8: With a fixed drive frequency, a shift in the resonant frequency will produce a phase shift in the response.

3.3 Installation

- Install new chamber with quadrupole in location Q15W
- Install heliax cables for microwave data
- Recover electronics from existing quadrupole detector and reinstall at new location
- Install a standard CESR chopper power converter for the new quadrupole

3.4 Commissioning

- With guidance from simulations, develop a program of measurements and experiments.
- Beam tests with electrons and positrons

3.5 Time Line

Assuming that funding is available summer 2015

- Summer 2015: Finalize the design of the shielded electrode flux detector and the RF design of the chamber.
- Fall 2015: Assemble and modify quadrupole laminations, assemble with spacers, wind coils and install support hardware.
- January 2016: Install new chamber with quadrupole in storage ring.
- April 2016: Detector commissioning and data taking.
- May 2016: Begin analysis

3.6 Data Taking and Analysis

Considerable effort will be required to develop the simulations to properly model the response of the electron flux detector and the resonant microwaves. The time-sliced particle-in-cell cloud buildup and electron macroparticle tracking numerical model, which includes photoelectron and secondary electron models as well as detector response functions, has proved essential in understanding the complicated relationship between the observed signals and the cloud spatial and time structures. Development of response modeling for the detector with improved azimuthal coverage will be necessary. Of particular interest will be the opportunity to validate the highly nonlinear relationship between signals and cloud density as a function of bunch population indicated by the modeling of existing measurements and predicted for the measurements proposed here.

A clearing bunch has been observed to modulate the density of the trapped cloud. We propose to develop experimental techniques to quantify this modulation by measuring the change in the sideband amplitude of resonant microwaves. We will also develop hardware and analysis that use direct phase detection so that the DC magnitude of the trapped cloud can be measured.

We will be taking data over a wide range of magnetic fields, with electrons for the first time as well as with positrons, and at different beam energies. In the past, large changes in magnetic field have always brought out either the inadequacies of the model or new physical insights. The analysis of the data from the flux and microwave detectors will proceed in parallel, with cross-calibration of the results of these two very different measurement techniques [15].

4 Broader Impact

The findings of the CESRTA electron cloud research program formed the basis for the design of the damping rings for the International Linear Collider[28][29]. Mitigations tested at Cornell 10 are being incorporated into the B-factory that is being built at KEK in Japan[30]. Evaluation of mitigations has informed the design of LHC upgrades where electron cloud effects are observed to limit the number of proton bunches that can be circulated in the collider[31]. Electron cloud trapped in the very high gradient interaction region quadrupoles has been identified as an important contribution to cryogenic head load[32]. The observation of trapped cloud in CESR prompted a collaborative study of the phenomenon in SuperKEK-B[33].

Accelerators deliver X-rays, produce high-energy particles and create the conditions found in the center of stars and the early stages of our Universe. By one estimate, between 1939 and 2009, a Nobel Prize was awarded every 2.9 years for research made possible or carried out at least partially on an accelerator [34]. By improving the performance of accelerators, this proposal will benefit all of these. It will also make them more cost effective to build and operate. Today's accelerators are also a critical tool for industry, medicine, national defense, and research, and may offer a path to safe nuclear energy. Annual sales of industrial accelerators, for example, exceed $2B, and are growing at an estimated 10% per year [35].

5 Outreach

Over the past several years, a number of undergraduate students have been involved in the acquisition and analysis of electron cloud data, many as part of the Research Experience for Undergraduates (REU) program. Some of the students who contributed to the study of trapped cloud and the development of the resonant microwave technique include Sean Foster, Lillie Pentecost, Ken Hammond, Robert Schwartz, Ben Carlson, Danielle Duggins, Alister Tencate, Chris Shill,

and Erika Cowan. Indeed, REU student Chris Schill alerted us to a peculiarity in our measurements that turned out to be the signature of trapping[36] and REU student Dante Iozzo's modeling study of trapped electrons led to the discovery and quantification of a highly nonlinear relationship between the observed signals and the cloud density[37]. Their names appear as authors and coauthors of many of the conference proceedings and publications. We look forward to the continued involvement of students at all levels, in this research.

6 Results from Prior Support

- NSF 1002467 Lepton Collider R&D 5/1/2011-4/30/2015

With prior support from both NSF and DOE, the CESRTA research program has made important contributions to our understanding of beam dynamics of ultra-low emittance storage rings, and to the development of instrumentation for measuring properties of the beam and its environment. The results appear in more than 150 conference proceedings, PhD theses, internal reports and peer reviewed journal articles. The compete bibliography of CESRTA publications is included, beginning on page 4, of the 'References Cited' section of this proposal

6.1 Electron Cloud

Our study of the electron cloud includes characterization of mitigations, measurement of cloud growth and decay, and investigation of the dynamics of the interaction of the circulating electron or positron beam with the cloud. Electron cloud simulation codes have been extended and refined based on comparisons with our extensive data set and have become a more reliable tool for predicting behavior. Specialized instrumentation was developed to enable many of the studies. Nearly 30 retarding field analyzers were deployed in different magnetic field and vacuum environments in the Cornell storage ring to measure the time averaged flux of electrons hitting the walls of the vacuum chamber. Shielded electrodes provided time resolved measurements of electron flux and a direct observation of cloud growth and decay. The density of the electron cloud in the volume of the chamber was measured by observing the cloud induced phase and frequency shift of resonant microwaves.

6.1.1 Retarding Field Analayzers

The retarding field analyzer (RFA) measures the DC flux of electrons into the wall of the vacuum chamber. It is the principle tool for measuring the growth of the cloud and the surface properties of the chambers, and for determining the effectiveness of various suppression techniques. The RFA is mounted on the top of the chamber and is typically segemented to provide position dependence. The voltage on the retarding grid determines the minimum energy electron that can reach the collector, thus providing a means of measuring the electron energy distribution [21]. A voltage scan with an RFA in a field free region is shown in Fig. 9. A comparison of RFA measurements for five different beam pipe coatings is shown in Fig. 10. Fig. 11 is an example of a dipole RFA data taken as a function of the magnetic field. The most prominent feature of the data is regularly occurring spikes or dips in all three plotted chambers. These correspond to "cyclotron resonances," which occur whenever the cyclotron period of cloud electrons in the dipole field is an integral multiple of the bunch spacing thus enhancing the transfer of energy from the beam to the electron. With 4 ns bunch spacing the data show resonant enhancement at intervals of 89 Gauss, in good agreement with our simple model. The resonances appear as peaks in the RFA signal in the Aluminum chamber,

but as dips in the coated chambers. The resonant enhancement in the uncoated aluminum vacuum chamber is a result of higher energy electrons striking the bottom and top of the vacuum chamber at more grazing angles. For TiN coated chambers, the energy dependence of the secondary yield peaks at lower energy than for aluminum. We find as a result that in the coated chambers the cloud density decreases on resonance, where the electron energy is beyond the peak yield. Simulations with the ECLOUD code that incorporate the appropriate physics parameters of the TiN coating are in good agreement with the measurements.

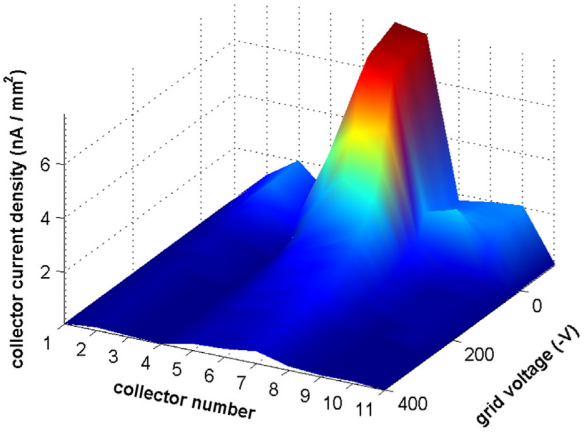

Figure 9: RFA voltage scan. The flux detector has 9 collectors arrayed across the top of the vacuum chamber, with collector 5 at the center. The electron cloud is evidently concentrated near the center of the chamber. The electron energy is given by $-V_{grid}$. The vacuum chamber is TiN coated, beam conditions $1 \times 45 \times 1.25$ mA, 5.3 GeV with 14 ns spaced bunches.

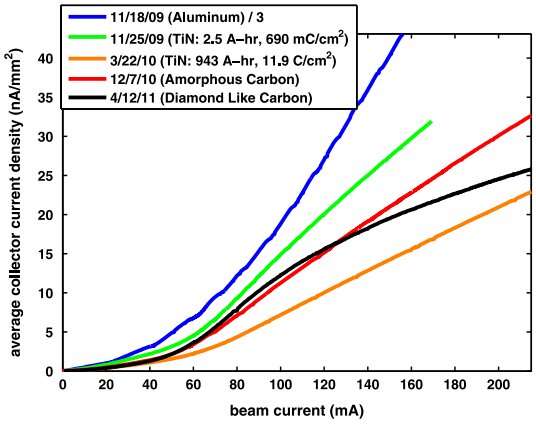

Figure 10: Comparison of different beam pipe coatings. Plots show average collector signal vs. beam current for 20 bunches of positrons with 14 ns spacing at beam energy 5.3 GeV. Note that the aluminum chamber signals are divided by 3. The TiN signal is plotted for two different beam doses.

6.1.2 Shielded Button Electrode

The shielded button electrode is a standard beam position monitor button electrode that is shielded from the direct beam signal by a screen with holes for transmission of cloud electrons. The time resolution of the detector is a fraction of a nanosecond permitting time-resolving measurements of the growth and decay of the cloud. In a typical measurement, two bunches are circulated in the storage ring. Synchrotron radiation from the lead bunch knocks electrons off the walls that then populate the chamber with some distribution. The trailing (witness) bunch of positrons kicks electrons that have drifted to the bottom half of the chamber into the detector at the top. The delay of the witness bunch with respect to the lead maps the development of the cloud.

The time evolution of the cloud is sensitive to its kinematic phase space distribution[18],[14]. The beam kicks, which can be controlled by varying the bunch population, accelerate cloud electrons to energies at and beyond the peak energy of the secondary emission curve. Subsequent collisions with the vacuum chamber wall reduce the cloud kinetic energy. Eventually the secondary emission process is dominated by elastic reflection of the remaining low-energy electrons. The cloud lifetime is then determined by the material-specific elastic yield value of the surface.

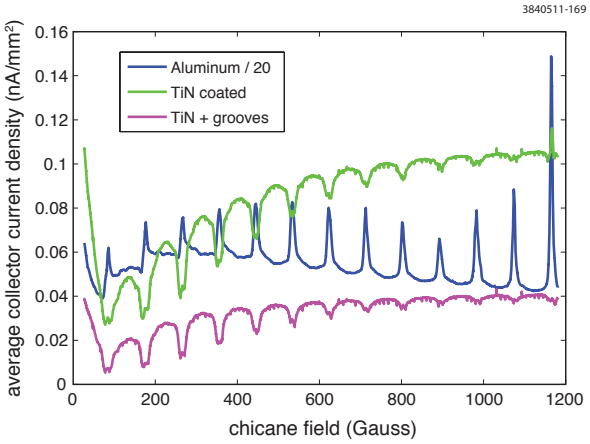

Figure 11: RFA signal as a function of dipole field: 1×451mA positrons, 5 GeV 4 ns spacing. Cyclotron resonances are observed every 89 G. Note that the Aluminum chamber signal is divided by 20.

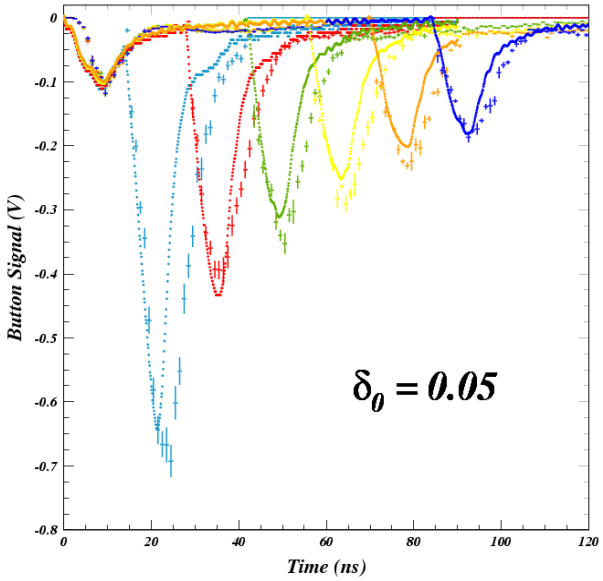

Figure 12: Witness bunch study with the TiN-coated aluminum chamber. The smooth curves show the digitized shielded electrode signals, while the points show the results of the model including statistical uncertainties.

Fig. 12 illustrates a method of determining cloud lifetime, and the elastic yield value, for a titanium nitride coated chamber. Overlaying the two-bunch signals obtained by varying the delay in the arrival of the trailing bunch in 14-ns steps clearly shows both the buildup and decay of the cloud. Six scope traces produced by two 5.3 GeV positron bunches of population 8×10^{10} are superposed. The delay of the witness bunch ranges from 14 to 84 ns. The magnitudes of the modeled signals at large witness bunch delay show the dependence on the elastic yield parameter δ_0. The best fit is given by a value $\delta_0 = 0.05$, which is an order of magnitude lower than is obtained from measurements on an uncoated aluminuum vacuum chamber. Detectors that combine the position and energy sensitivity of the RFA with the temporal measurement of the shielded detector, have been installed in dipole and quadrupole chambers.

Measurements of the electron cloud with resonant microwaves are shown in Fig. 13. If the EC density were uniform over the length of this section of beam-pipe, the data obtained from these five resonances would coincide. But at the highest current, the measured EC densities vary by about 30%. The differences in these measurements are too large to be explained by errors in the measurement of the Q of each resonance or of the sideband ratios, suggesting that the EC density is not uniform and that the distribution of the standing waves is not symmetric. Indeed the asymmetry of the standing waves provides a means for measuring the nonuniformity of the cloud[19].

6.1.3 Electron Cloud Beam Dynamics

Experiments were performed at CESRTA to characterize the interaction of the electron cloud with the high energy positron and electron beams. The first order effect of the electron cloud on the circulating beam is to focus positron beams and defocus electron beams. The focusing (defocusing) is manifested as a tuneshift. A train of bunches produces an electron cloud with density increasing

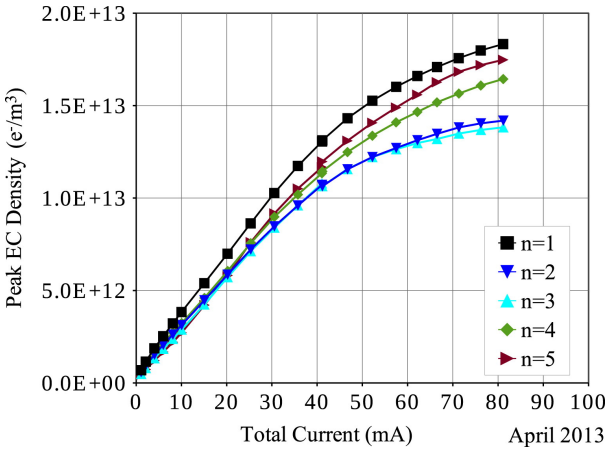

Figure 13: The EC density is calculated for each of the five peak frequencies iof Fig. 7 and plotted as function of total beam current in a 10-bunch train of positrons.

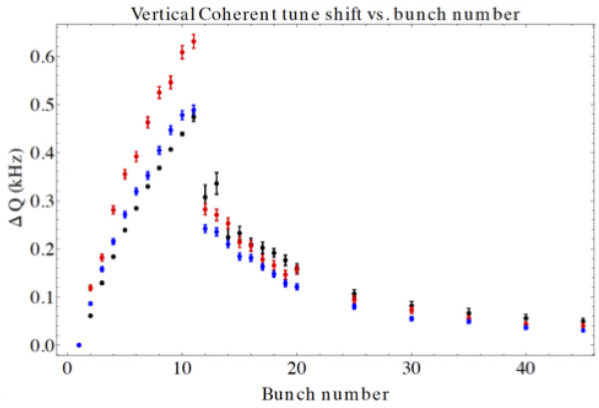

Figure 14: Measured tune shifts (black points) vs. bunch number, for a train of 10, 0.75 mA, 5.3 GeV positron bunches with 14 ns spacing, followed by witness bunches. Blue points are from POSINST simulation and a sophisticated model of synchrotron radiation.

along the train[22]. The tune is shifted for each bunch by an amount proportional to the local cloud density. A measurement of the bunch by bunch tune shift for a train of ten bunches is shown in Fig. 14. The points in the figure at bunch numbers greater than 10 are measurements for the tune shift of a witness bunch placed sequentially in 14 ns increments beyond the end of the train to characterize the decay of the cloud. In Fig. 15 the electron density as determined by the measured tune shift for a train of 30 bunches is plotted along with the results of the POSINST simulation of the density. A second order effect of the cloud on the beam is to increase the beam emittance. Beam centroid motion and size are observed to grow along a train. Often the first bunch in the train has an anomalously large size. Fig. 16 shows the measured vertical size and centroid motion of each bunch in a train of 30 positron bunches. A quantitative understanding of the physics driving these effects is the subject of ongoing research.

6.2 Instrumentation

The beam based measurements essential to the research program required the development of new instrumentation, including a multi-bunch multi-turn beam position monitor system, an X-ray beam size monitor for bunch by bunch measurement of vertical beam size, a visible light monitor of horizontal beam size, and a digital tune tracker for resonantly driving individual bunches at the normal mode frequencies.

6.2.1 X-Ray Beam Size Monitor

The X-ray beam size monitor[25] measures bunch by bunch and turn by turn vertical beam size with resolution of a few microns. Synchrotron X-rays radiated by the bunch in a hard bend magnet are imaged by an optical element onto a detector.

The fast diodes and readout provide turn by turn measurement of the size of bunches separated by as few as 4 ns. That capability is illustrated in Fig. 16 that shows beam size as a function of bunch number for 30 bunches with 4 ns spacing, preceded by a precursor bunch 20 ns ahead of the

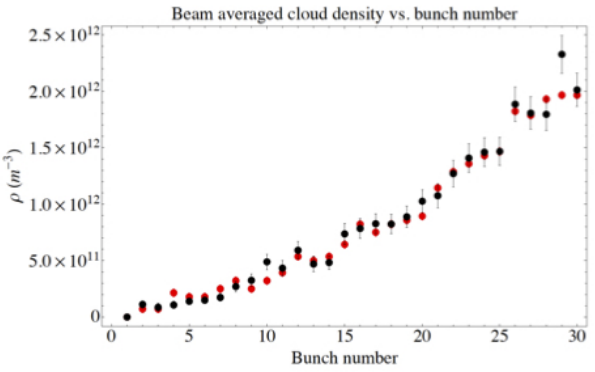

Figure 15: Average initial (i.e., before the "pinch") electron cloud density vs. bunch number, com- parison between estimate from measured tune shifts (red), and simulation (black) from POSINST.

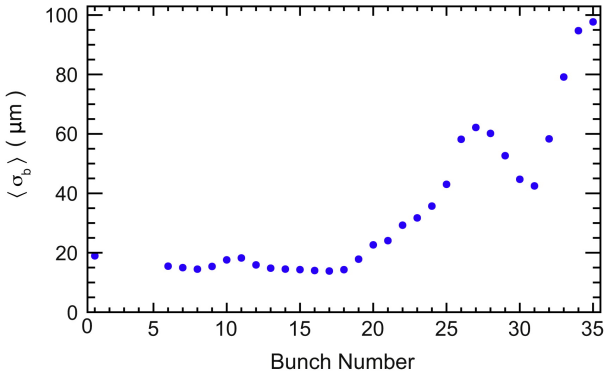

Figure 16: Turn-averaged beam size by bunch number for a run with 30 bunches in a train with 4 ns bunch separation and an additional precursor bunch 20 ns ahead of the train.

train. The precursor is meant to temporarily sweep away the electron cloud. Without the precursor we find that the lead bunch (bunch #6) tends to have larger beam size. A coded aperture optic, optimized for operation in the low beam energy regime (1.8GeV) where the X-ray spectrum is soft and the photon statistics limited, was successfully tested, demonstrating a significantly improved resolving power. The new optic was used for measurements of intra-beam scattering[26].

6.2.2 Visible Light Beam Size Monitor

A beam profile monitor utilizing visible synchrotron radiation (SR) from a bending magnet has been designed and installed in the storage ring (CESR)[24]. The monitor employs a double-slit interferometer, as shown in Fig. 17 to measure both the horizontal and vertical beam sizes over a wide range of beam currents. By varying the separation of the slits, beam sizes ranging from 50 to 500 μm can be measured with a resolution of approximately 5 μm. By imaging the π-polarized component of SR, a small vertical beam size ($\sim$ 70 μm) was measured during an undulator test run in CESR, which was consistent with the interferometer measurement. To measure the bunch length, a beam splitter is inserted to direct a fraction of light into a streak camera setup. This beam size monitor measures the transverse and longitudinal beam sizes simultaneously, a capability that has proven invaluable for the study of collective effects that dilute the beam emittance. A measurement of the dependence of the horizontal beam size on bunch charge is shown in Fig. 18 along with the prediction of intra-beam scattering (IBS) theory. As anticipated, the increase in horizontal beam size due to IBS depends on the initial ($\sim$zero current) vertical emittance[26].

6.3 Low Emittance Tuning

The low emittance tuning algorithm developed at CESRTA [27] routinely achieves geometric vertical emittance of order 10 pm-rad and is limited by survey tolerances. The tuning algorithm depends on beam based measurements of the closed orbit, transverse coupling, and vertical dispersion. The coupling is determined by resonantly exciting a bunch at the transverse normal mode tunes, and measuring out of plane response at each BPM. Dispersion is similarly determined by exciting the beam at the synchrotron tune and measuring horizontal and vertical response at that frequency. A digital tune tracker [39] is used to drive the beam on resonance and to monitor the phase of the

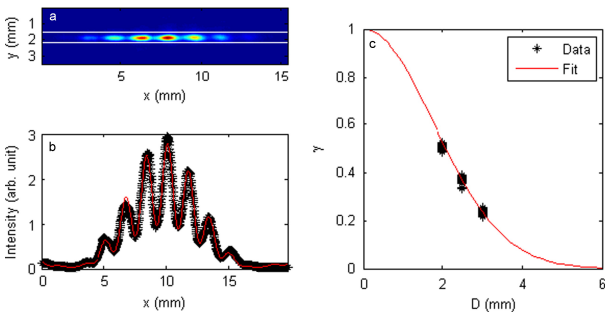

Figure 17: A typical interference pattern of SR using a D=2.0 mm double slits. (b) The horizontal intensity profile integrated between two white lines in (a) and the best fit using Eq. (1). (c) The visibility measured using three different sets of double slits (D=2.0, 2.5, and 3.0 mm).

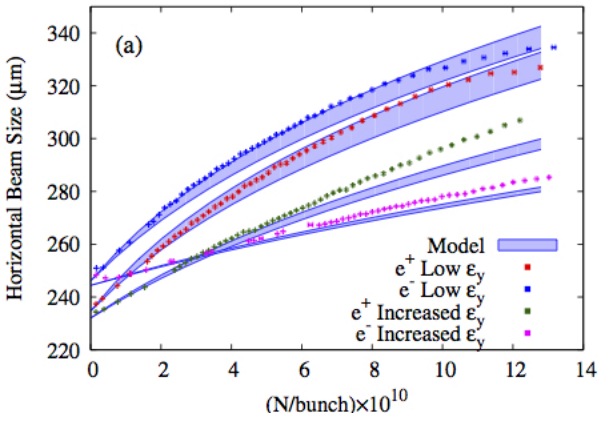

Figure 18: Horizontal beam size vs bunch charge for electrons and positrons at low vertical emittance and then again with higher vertical emittance. The points are the data and the bands the model of intra-beam scattering including theoretical uncertainty.

drive on each turn for comparison with the measured phase of the bunch at each BPM. Because the data is collected in a fraction of a second, the emittance tuning technique is insensitive to drifts in timing and BPM gain. Insofar as no guide field magnets need be changed, the method is relatively non-destructive.

6.4 Collective effects

The instrumentation described above has enabled the study of other collective effects, including intra-beam scattering (see Fig. 18)[26] and the fast ion instability [40].

6.5 Publications

The complete bibliography of reports, conference proceedings and peer reviewed publications documenting the results of prior support for the CESRTA research program appears beginning on page 4 of the 'References Cited' section of this proposal. A number of analysis and simulation codes have been developed as part of the research program. The *BMAD* [41] open source code library now includes modules for computing, fast ion instability, intra-beam scattering, wakefield effects, space charge. The CMAD [42] simulation is used to study the interaction of the beam with the electron cloud and has reproduced a number of the features of the data.